THE STRUCTURAL, MECHANICAL, ELECTRONIC AND OPTICAL PROPERTIES OF AMn_7O_{12} (A= Ca, Cd, Sr) PEROVSKITE COMPOUNDS

YILMAZ ŞENER[1], HUSNU KOC[2], AMIRULLAH M. MAMEDOV[3,4], EKMEL OZBAY[3]

[1]*Department of Physics, Faculty of Science and Letters, Siirt University, Siirt, Turkey*
[2]*School of Health, Safety and Health at Work, Siirt University, 56100, Siirt, Turkey*
[3]*Nanotechnology Research Center, Bilkent University, Bilkent, Ankara, Turkey*
[4]*Baku State University, International Scientific Center, Baku, Azerbaijan*
e:mail: hkoc@siirt.edu.tr

The structural, mechanical, electronic, and optical properties of rhombohedral AMn_7O_{12} (A=Ca, Cd, and Sr) compounds are investigated using spin polarized generalized gradient approximation (GGA) for the exchange-correlation energy. For $CaMn_7O_{12}$, $CdMn_7O_{12}$, and $SrMn_7O_{12}$ compounds, the difference between the experimental lattice parameter values used in the calculations and the values obtained as a result of the structural optimization is less than 1%, 1.5%, and 1.4%, respectively. It has been observed that the elastic constants calculated using the stress-strain relationship meet the Born stability criteria for the rhombohedral structure. The elastic modulus and other related quantities have also been calculated and interpreted from these elastic constants. In the spin polarized state, all three compounds have a semi-metal electronic band structure. Finally, the real and imaginary parts of the frequency dependent dielectric function along the x and z axes and other optical functions have been calculated.

Keywords: electronic structure, mechanical properties, optical properties, density functional theory
PACS: 71.20.−b; 62.20.−x; 74.25.Gz; 71.15.Mb

1. INTRODUCTION

The compounds with the general formula $(AA'_3)B_4O_{12}$ (A=Ca, Cd, Na, Sr, and rare earth elements), where the A' (Mn, Co, Pd, Cu) and B (B=Mn, Fe, Cr, Al vb) cations are very close to each other, produce fundamental physics to understand the coupling mechanism of static electricity and magnetism. Moreover, these compounds have attracted great interest in various technological applications due to their interesting physical properties, such as heavy fermion properties, intersite charge transfer, structural phase transitions, giant dielectric constant, linear and nonlinear magnetic order, and multiferroic properties [1-3].

Among AMn_7O_{12} perovskite compounds, the rhombohedral $CaMn_7O_{12}$ compound has received much attention due to its preparation at ambient pressure/or room temperature and its magnetically induced giant ferroelectric polarization (Ps ~ 2870 $\mu C/m^2$) [1-5]. When the compound $CaMn_7O_{12}$ is annealed at 450-462 K, it exhibits a structural phase transition from a rhombohedral ($R\bar{3}$) to cubic (space group $Im\bar{3}$) structure. $CdMn_7O_{12}$ and $SrMn_7O_{12}$ compounds have been investigated recently because their structural and physical properties can be prepared at high pressures and temperatures [2-9]. Most of the AMn_7O_{12} (A=Ca, Cd, La, Na, Nd, and Sr) perovskites were studied by Marezio et al. [10] in the 1970s and subsequently extensively studied due to their complex magnetic orders and structural transitions. In the literature review, it was shown that only the electronic properties of the $SrMn_7O_{12}$ compound among these complex compounds have been examined theoretically [11].

As far as we know, the physical properties of these compounds have not been studied theoretically until now, except for the electronic properties of $SrMn_7O_{12}$. In this study, this gap will be filled since the physical properties (structural, mechanical, electronic, and optical properties) of AMn_7O_{12} (A=, Ca, Cd, Sr) perovskite compounds will be examined using the ab-initio method.

2. METHOD

In all of our calculations that were performed using the ab-initio total-energy and molecular-dynamics program VASP (Vienna ab-initio simulation program) [12-15] that was developed within the density functional theory (DFT) [16], the exchange-correlation energy function is treated within the spin polarized GGA (generalized gradient approximation) by the density functional of Perdew et al. [17]. The potentials used for the GGA calculations take into account the $3p^64s^2$ valence electrons of each Ca-, $4d^{10}5s^2$ valence electrons of each Cd-, $4p^65s^2$ valence electrons of each Sr-, $3d^54s^2$ valence electrons of each Mn-, and $2s^22p^4$ valence electrons of each O-atoms. When including a plane-wave basis up to a kinetic-energy cutoff equal to 21.17 Ha for $CaMn_7O_{12}$ and 19.55 Ha for $CdMn_7O_{12}$/$SrMn_7O_{12}$, the properties investigated in this work are well converged. The Brillouin-zone integration was performed using special k points sampled within the Monkhorst-Pack scheme [18]. We found that a mesh of 7x7x3 k points for C2/c, 5x5x4 k points for C2/m, and 6x3x6 k point for $P2_1/m$ was required to describe the structural, mechanical, electronic, and optical properties. This k-point mesh guarantees a violation of charge neutrality less than 0.008e. Such a low value is a good indicator for an adequate convergence of the calculations.

3 RESULT AND DISCUSSION

3.1 STRUCTURAL PROPERTIES

The unit cell structure of AMn_7O_{12} (A=Ca, Sr, Cd) compounds is given in Figure 1. Here, Sr, Mn, and O ions are represented by blue, green, and red colors, respectively. There are three different symmetry regions for Mn ions, labeled Mn_1, Mn_2, and Mn_3. The Mn_1 ions occupied the 9e (0.5, 0, 0) regions, Mn_2 ions 9d (0.5, 0, 0.5) regions, and Mn_3 ions 3b (0, 0, 0.5) regions [4]. It is determined that these materials have an R-3 space group at room temperature and 60 atoms (3 AMn_7O_{12} molecules) in their unit cell.

By using the experimental lattice parameter values given in Table 1 and the atomic positions given in Ref [4, 11, 19], a rhombohedral (R-3) unit cell structure was created for AMn_7O_{12} compounds and the optimization process was performed. As a result of the optimization process, the lattice parameter values of AMn_7O_{12} compounds were calculated. The results that we obtained are given in Table 1 together with the experimental and theoretical results. The differences between the experimental values [1-4, 8, 11, 19-21] that we used in the calculations and the values we calculated are less than about 1.5% for $CaMn_7O_{12}$, less than about 1% for $CaMn_7O_{12}$, and less than about 1.4% for $SrMn_7O_{12}$. This shows that the lattice parameter values that we obtained are reliable and applicable in calculating the physical properties (mechanical and electronic) of AMn_7O_{12} (A=Cd, Sr) compounds.

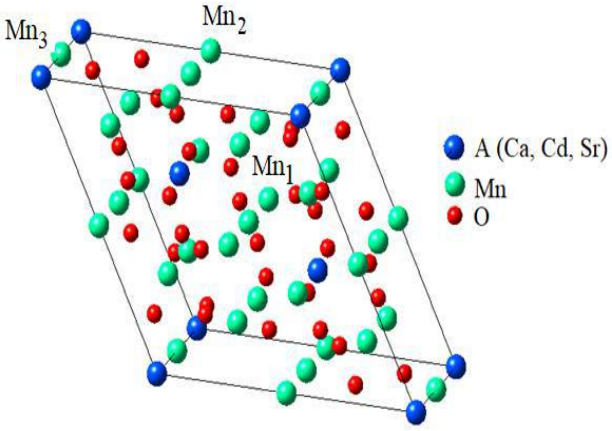

Fig. 1. The rhombohedral crystal structure of AMn_7O_{12} (A=Ca, Sr, Cd).

Table 1.
The calculated equilibrium lattice parameters (a and c) together with the experimental and theoretical values for AMn_7O_{12} (A= Ca, Sr, Cd) compounds

.

Compounds	a (Å)	c (Å)	V_0 (Å^3)	References
$CaMn_7O_{12}$	10.435	6.432	606.52	Present
	10.443	6.343	599.11	Exp. [20]
	10.442	6.343		Exp. [4]
	10.441	6.340		Exp. [1]
	10.459	6.343	600.86	Exp. [3]
	10.440	6.340		Exp. [8]
	10.630	6.31		Exp. [21]
$CdMn_7O_{12}$	10.455	6.395	605.29	Present
	10.453	6.336	599.56	Exp. [19]
	10.455	6.331	599.35	Exp. [2]
	10.431	6.318		Exp. [7]
$SrMn_7O_{12}$	10.555	6.465	623.79	Present
	10.509	6.384	610.59	Exp. [19]
	10.498	6.380		Exp. [1]
	10.498	6.380	608.92	Exp. [19]
	10.527	6.391		Teori (GGA) [11]

Table 2.
Magnetic moment values of Mn_1, Mn_2 and Mn_3 ions

Magnetic moment	Compounds	Mn_1	Mn_2	Mn_3	References
μB/f.u	$CaMn_7O_{12}$	3.631	3.362	-2.253	Present
		2.31	2.33	2.01	Exp. [22]
	$CdMn_7O_{12}$	3.442	-3.371	2.374	Present
	$SrMn_7O_{12}$	3.675	3.397	2.93	Present
		3.69	3.55	2.93	Teori (GGA) [11]

As a result of spin polarization calculations, magnetic moment values are obtained for AMn_7O_{12} (A=Ca, Sr, Cd) compounds. The magnetic moment values of Mn ions, which contribute the most to the magnetic moments of these compounds, are given in Table 2. When the Mn_1^{+3}, Mn_2^{+3} and Mn_3^{+4} magnetic moment values obtained for the $CaMn_7O_{12}$ compound are compared with the experimental values [22] given

in Table 2, the values of $Mn_1^{+3}$and $Mn_2^{+3}$are slightly larger than the experimental values, while Mn_3^{+4} is compatible in magnitude in opposite direction. The Mn_1^{+3}, Mn_2^{+3}, and Mn_3^{+4} values obtained for the $SrMn_7O_{12}$ compound are 3.675, 3.397 and 2.93, respectively. When these values are compared with the theoretical values [11], it is seen that they are all in agreement.

3.2. MECHANICAL PROPERTIES

The elastic constants are very important parameters to describe the properties of a material. It provides important information about the structural stability, hardness, ductility, nature of bonding between adjacent atomic planes, anisotropy and Debye temperature of materials [23]. In this study, the "stress-strain" method [24] has been used to calculate the elastic constants. The rhombohedral crystal system has six different elastic constants. The elastic constants C_{11}, C_{12}, C_{13}, C_{33}, C_{44}, and C_{66} were calculated and the results are given in Table 3. The elastic constants calculated for AMn_7O_{12} (A=Ca, Cd, Sr) compounds provide the Born stability criteria [25] for the rhombohedral structure. The elastic constants C_{11}, C_{22}, and C_{33} are used to test resistance to linear compression in the x direction [100], y direction [010], and z direction [001], respectively.

Table 3.
The calculated total elastic constants (in GPa) for AMn_7O_{12} (A= Ca, Sr, Cd) compounds.

Compounds	C_{11}	C_{12}	C_{13}	C_{33}	C_{44}	C_{66}
$CaMn_7O_{12}$	267.4	105.9	108.9	276.1	80.8	73.7
$CdMn_7O_{12}$	242.6	136.2	137.7	278.6	52.7	48.2
$SrMn_7O_{12}$	296.6	132.4	121.7	282.4	82.6	81.4

It is $C_{11}=C_{22}$ due to the rhombohedral structure. Considering the calculated C_{11} and C_{33} values, it is $C_{33}>C_{11}$ in $CaMn_7O_{12}$ and $CdMn_7O_{12}$ compounds, and $C_{11}>C_{33}$ in $SrMn_7O_{12}$ compounds. These results show that $CaMn_7O_{12}$ and $CdMn_7O_{12}$ compounds are more resistant to linear compression in the z direction, while $SrMn_7O_{12}$ is more resistant to linear compression in the x direction. Since the C_{11} and C_{33} values of $SrMn_7O_{12}$ are greater than the values of the other two compounds, this compound is less compressible in the x and z directions. The large elastic constants C_{44} and C66 relate to a strong resistance to shear distortions in the (100) plane and in the <110> direction, respectively. The calculated C_{44} and C_{66} values for the $SrMn_7O_{12}$ compound are 82.6 and 81.4, respectively. These values are greater than the values obtained for the other two compounds.

Bulk (B) and shear modulus (G), expressing the hardness of a material, can be obtained from elastic constants. We used the Voigt, Reuss, and Hill approximation [26-28] to calculate the bulk and shear modulus of AMn_7O_{12} (A=Ca, Cd, Sr) compounds. Then, other quantities (Young modulus, Poisson ratio, B/G ratio, anisotropic factors, sound velocities, and Debye temperature) were calculated using elastic constants, bulk modulus, and shear modulus values. The calculation results are given in Table 4.

Table 4.
The calculated isotropic bulk modulus (B, in GPa), shear modulus (G, in GPa), Young's modulus (E, in GPa), and Poisson's ratio for AMn_7O_{12} (A= Ca, Sr, Cd) compounds.

Compounds	B_R	B_V	B_H	G_R	G_V	G_H	E	υ	B/G
$CaMn_7O_{12}$	161.97	162.03	162.00	77.95	78.13	78.04	201.73	0.292	2.076
$CdMn_7O_{12}$	175.52	176.33	175.93	52.89	53.20	52.89	144.22	0.363	3.326
$SrMn_7O_{12}$	180.52	180.80	180.54	82.46	82.50	82.48	214.75	0.302	2.190

The Bulk modulus (B) represents the ratio of the stress- strain applied to the unit volume, while the Shear modulus (G) represents the ratio of the stress- strain applied to the unit surface. Young's modulus (E) is the ratio between stress-strain and reflects the material's ability to resist strain [29]. As can be seen in Table 4, the largest and smallest bulk modulus values are obtained as 180.54 GPa for $SrMn_7O_{12}$ and 162.00 GPa for $CaMn_7O_{12}$, respectively, while the largest and smallest shear modulus values were obtained as 82.48 GPa for $SrMn_7O_{12}$ and 52.20 GPa for $CdMn_7O_{12}$, respectively. Among the three compounds, SrMn7O12 has the highest Young's modulus value. Therefore, the SrMn7O12 compound is a harder material than other compounds. The Poisson's ratio reveals the nature of mechanical bonds as well as the interatomic forces in various bonds [30-32]. Poisson's ratio of $\upsilon = 0.1$ indicates that covalent bonds dominate in the solid, while $\upsilon = 0.25$ indicates that ionic bonds dominate. The υ values for the compounds $CaMn_7O_{12}$, $CdMn_7O_{12}$, and $SrMn_7O_{12}$ are 0.292, 0.363 and 0.302, respectively. It is seen that the ionic contribution is dominant in all three compounds, but the contribution in the $CdMn_7O_{12}$ compound is slightly higher than the other two compounds. The B/G ratio can be used to determine whether a material is brittle (B/G <1.75) or ductile

(B/G>1.75) [33, 34]. The B/G value of all three materials is more than 1.75. When Table 4 is examined, it will be seen that the $CdMn_7O_{12}$ compound is a more ductile material than the other two compounds.

The elastic anisotropy is an important physical parameter related to the mechanical properties of solids. Anisotropy factors for rhombohedral compounds are $A_1=2C_{66}/(C_{11}-C_{12})$ for (100) planes and $A_3=4C_{44}/(C_{11}+C_{33}-2C_{13})$ for (001) planes [35]. If the value of the anisotropy factors is equal to 1, the material is isotropic, and if it is greater or less than 1, it has anisotropic character. When Table 5 is examined, it is seen that the A_1 and A_2 values of the $CdMn_7O_{12}$ compound are less than 1 compared to the other two compounds.

Therefore, this compound has more anisotropic character than the other two compounds. The elastic bulk and shear modulus also contribute to anisotropy.

Table 5.

The calculated anisotropic factors, sound velocities ($\upsilon_t, \upsilon_l, \upsilon_m$), and the Debye temperatures for AMn_7O_{12} (A= Ca, Sr, Cd) compounds.

Compounds	A_1	A_3	A_B	A_G	v_t(m/s)	v_l (m/s)	v_m (m/s)	θ_D (K)
$CaMn_7O_{12}$	0.992	0.913	0.019	0.114	3926	7248	4381	870
$CdMn_7O_{12}$	0.865	0.905	0.250	0.593	3054	6593	3440	684
$SrMn_7O_{12}$	0.991	0.976	0.070	0.024	3943	7401	4406	867

The percentages of elastic A_B and A_G anisotropy due to linear bulk and shear stress are calculated using the $A_B=(B_V-B_R)/(B_V+B_R)x100$ and $A_G=(G_V-G_R)/(G_V+G_R)x100$ equations [36, 37]. The elastic A_B and A_G anisotropy percentages are zero for isotropic materials and different from zero for anisotropic materials. 100% corresponds to the highest anisotropy value. As can be seen in Table 5, the $CdMn_7O_{12}$ compound has the largest A_B and A_G values. Consistent with the above result, the compound $CdMn_7O_{12}$ has the most anisotropic character.

The Debye temperature is the characteristic temperature of a material at which the atoms have maximum modes of oscillation with respect to their equilibrium positions. Elastic vibration is caused by acoustic vibration mode at low temperature limit. At low temperature, the Debye temperature (θ_D (K)) and elastic wave velocities (transverse (υ_t), longitudinal (υ_l), and mean (υ_m)) were calculated using the equations in Ref [38-40]. The results are given in Table 5. When Table 5 is examined, it is seen that the $CdMn_7O_{12}$ compound has the highest Debye temperature value.

3.3. ELECTRONIC PROPERTIES

The electronic band structure gives the shape of the energy distributions of electrons and holes in a crystal structure. The fundamental properties of a material are determined by its electronic band structure. Since the calculated compounds have magnetic properties, the electronic structure calculations are made in the spin polarized state. In this study under zero pressure, electronic band structures of AMn_7O_{12} (A=Ca, Sr, Cd) compounds have been calculated along different high symmetry points (Γ (0,0,0)→L (0,1/2,0)→Z (1/2,1/2,1/2)→Γ (0,0,0)). The spin up and spin down electronic band structures obtained as a result of the calculation and the partial state densities (PDOS) corresponding to these band structures are given in the Figure 3-Figure 6. The horizontal dashed lines in the figures are the Fermi energy level (E_F).

The electronic band structures calculated in the spin polarized state are given in Figure 2. Figure 2 shows that all three compounds have a semi-metal structure. We obtained this result for the $SrMn_7O_{12}$ compound and it is in agreement with the result stated by Liu et al. [11]. Considering the spin up and spin down electronic band structures (See Figure 3) calculated for all three compounds, the compounds $CaMn_7O_{12}$ and $SrMn_7O_{12}$ in the spin up state and the $CdMn_7O_{12}$ compound in the spin down state are in semi-metal structure. When the spin down band graph for the $CaMn_7O_{12}$ compound is examined, it is seen that the maximum of the valence band is at the L point while the minimum of the conduction band is at the Γ point. Therefore, the transitions between the bands are indirect and the calculated E_g value is 1.227 eV.

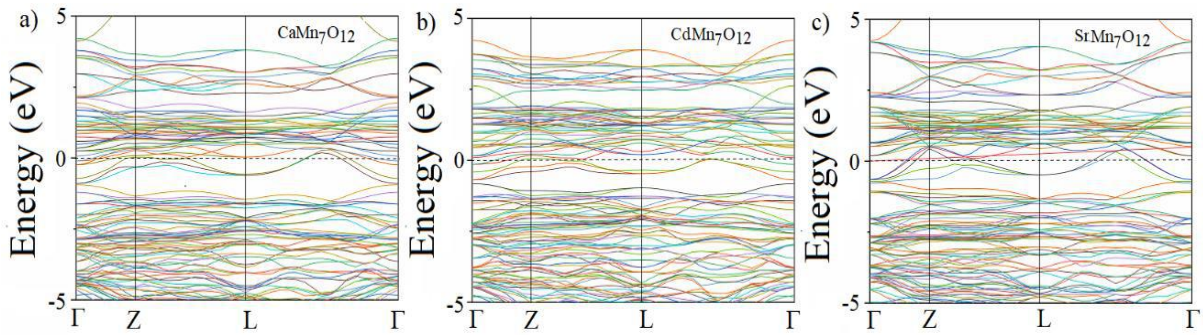

Fig. 2. Electronic band structures calculated for a) $CaMn_7O_{12}$, b) $CdMn_7O_{12}$, and c) $SrMn_7O_{12}$ in the spin

polarized state.

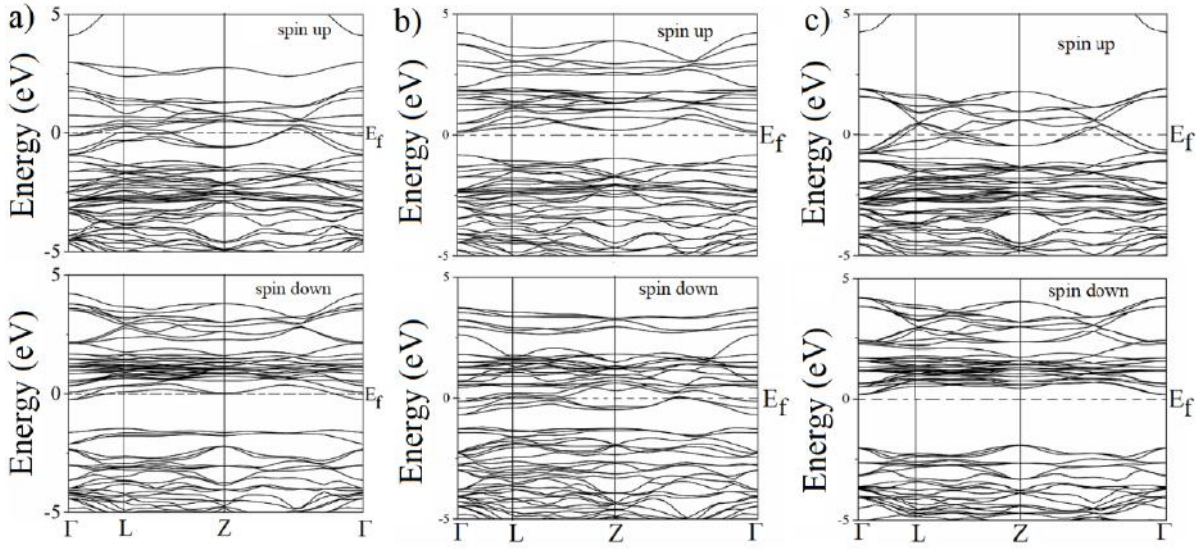

Fig. 3. The calculated electronic band structures for the spin up and spin down of a) $CaMn_7O_{12}$, b) $CdMn_7O_{12}$, and c) $SrMn_7O_{12}$ compounds.

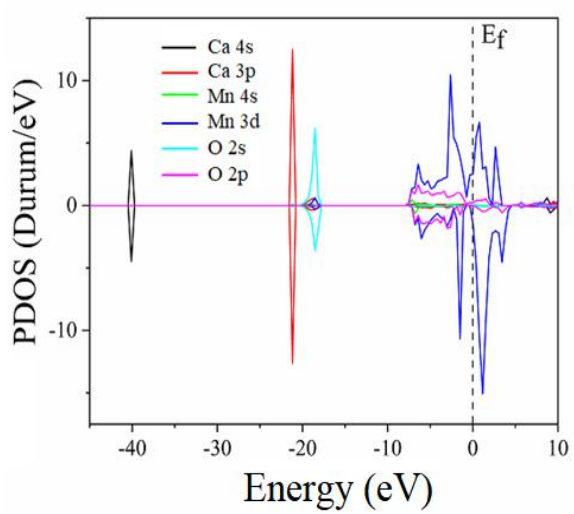

Fig. 4. The projected density of states for the $CaMn_7O_{12}$ compound.

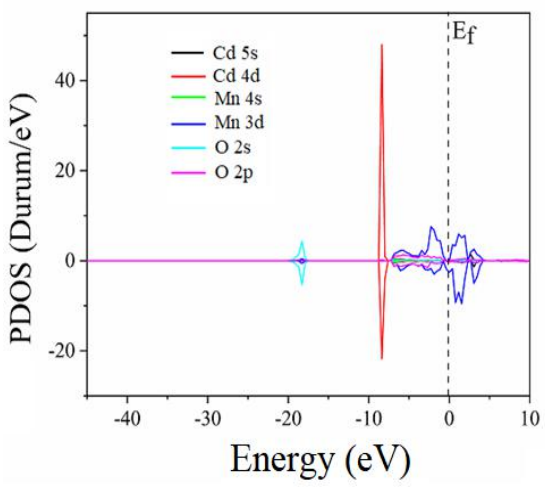

Fig. 5. The projected density of states for the $CdMn_7O_{12}$ compound.

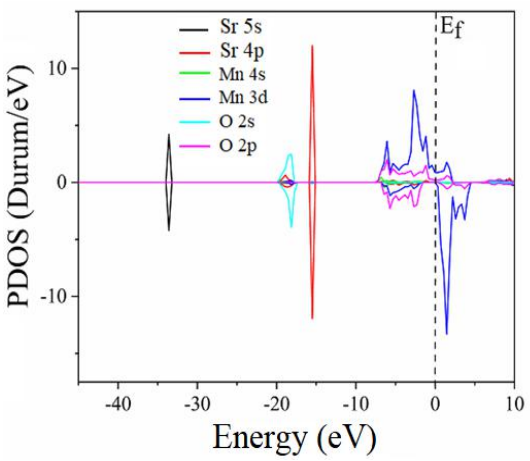

Fig. 6. The projected density of states for the $SrMn_7O_{12}$ compound.

When the spin up band graph for the $CdMn_7O_{12}$ compound is examined, it is seen that the maximum of the valence band and the minimum of the conduction band are at the same k-point, that is, at the Γ point. In the spin up state, the transitions between bands are direct and the calculated E_g value is 0.917 eV. In the spin down band graph of $SrMn_7O_{12}$, the maximum of the valence band and the minimum of the conduction band are at the Γ point, as in the spin up graph of $CdMn_7O_{12}$. Therefore, the transitions between the bands are direct and the calculated E_g value is 2.214 eV.

The spin-dependent partial density of states corresponding to the electronic band structures of $CaMn_7O_{12}$, $CdMn_7O_{12}$, and $SrMn_7O_{12}$ compounds are given in Figure 4, Figure 5, and Figure 6, respectively.

When Figure 4 is examined, in both spin states, the contribution to the lowest valence bands (-45-40 eV) comes from Ca 4s states, the contribution to the bands just above these bands comes from Ca 3p, and the contribution to the bands between -20-15 eV comes

mainly from O 2s states, although the contribution of other states is small. Although the contribution of O 2p states to the valence bands just below the Fermi level (-8-0 eV) and the conduction bands just above it in both spin states cannot be ignored, it is seen that the main contribution comes from the Mn 3d states. This means that there is relatively strong p-d hybridization in the bands. When Figure 5 is examined, in both spin states, the highest contribution to the lowest valence bands comes from the O 2s states and the contribution to the bands just above it comes from the Cd 4d states. Although the contribution of O 2p states to the valence bands just below the Fermi level (-8-0 eV) and the conduction bands just above it in both spin states is very small, it is seen that the predominant contribution comes from Mn 3d states. In these bands, it means that there is weak p-d hybridization. Finally, when Figure 6 is examined in both spin states, the contribution to the lowest valence bands (-35-30 eV) comes from the Sr 5s states, the contribution to the bands just above these bands comes mainly from the O 2s states, although the contribution of the other states is small, and the contribution to the bands between -20-15 eV comes from the Sr 4p states. As in the $CaMn_7O_{12}$ compound, although the contribution of O 2p states to the valence bands just below the Fermi level (-8-0 eV) and the conduction bands just above it in both spin states cannot be ignored, it is seen that the main contribution comes from the Mn 3d states. This means that there is also relatively strong p-d hybridization in these bands.

3.4. OPTICAL PROPERTIES

Optical properties are studied to predict how a material will behave when exposed to electromagnetic radiation. The optical response of a material exposed to radiation is a function of energy or a range of frequencies. Optical properties are related to the electronic band structure of the material. Interactions between a charge carrier on the surface of the material and incident photons cause optical properties to emerge. First, the imaginary part of the dielectric function ($\varepsilon_2(\omega)$) is calculated from the band structure of the materials. Then, the real part of the dielectric function ($\varepsilon_1(\omega)$) is obtained from $\varepsilon_2(\omega)$ using the Kramers-Kronig relationship [41, 42]. Other optical properties are calculated using the

Due to the symmetry of the rhombohedral structure, the real ($\varepsilon_1(\omega)$) and imaginary parts ($\varepsilon_2(\omega)$) of the dielectric function for AMn_7O_{12} (A=Ca, Sr, Cd) compounds were calculated in the x and z directions. Data between 0 and 120 eV was obtained for the real and imaginary parts of the dielectric function, but it was deemed appropriate to use data between 0 and 12 eV in graphic drawings. The calculation results are given in Figure 7-Figure 9. As can be seen in the figures, the real part of the dielectric function takes zero values in transitions from a positive value to negative value ($(d\varepsilon_1)/dE<0$) and from negative value to positive value ($(d\varepsilon_1)/dE>0$). The values of ε_1 in the x- and z-directions are given in Table 6. These values are the values where the reflection decreases.

Table 6.
Some of the principal features and singularities of the linear optical responses for AMn_7O_{12} (A= Ca, Sr, Cd) compounds.

Compounds	$\varepsilon_1(eV)$	$d\varepsilon_1/dE<0$			$d\varepsilon_1/dE>0$			$\varepsilon_2^{maks}(eV)$	
$CaMn_7O_{12}$	ε_1^x	0.246	20.456	27.026	11.158	21.571	29.506	ε_2^x	0.372
	ε_1^z	0.246	20.332	27.150	11.282	23.103	29.506	ε_2^z	0.372
$CdMn_7O_{12}$	ε_1^x	0.374	5.245		0.874	7.119		ε_2^x	0.249
	ε_1^z	0.249	5.120		1.373	6.994		ε_2^z	0.249
$SrMn_7O_{12}$	ε_1^x	0.245	10.122	22.837	8.887	10.493	26.663	ε_2^x	0.123
	ε_1^z	0.245	10.246	22.960	8.887	10.493	26.663	ε_2^z	0.123

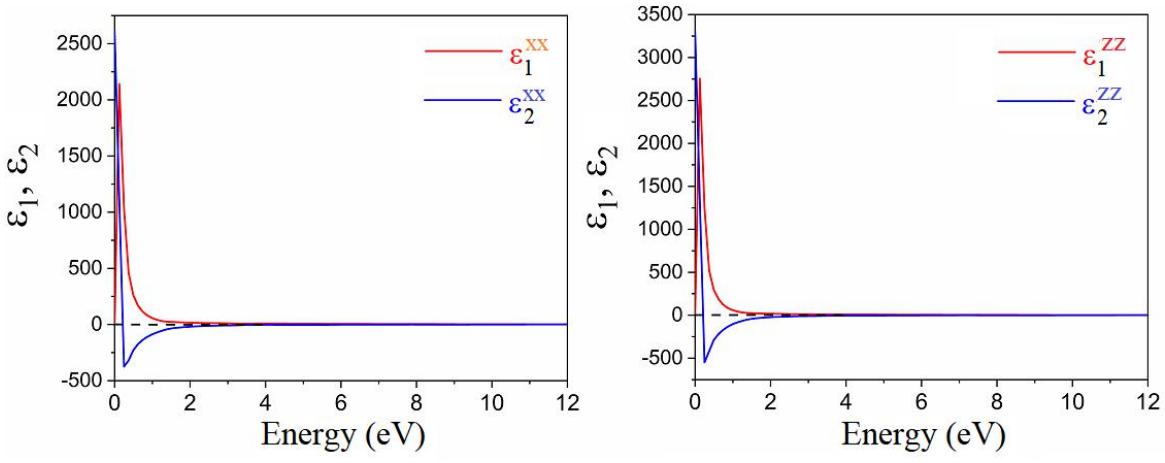

Fig. 7. The calculated reel and imaginary parts of dielectric functions for the $CaMn_7O_{12}$ compound.

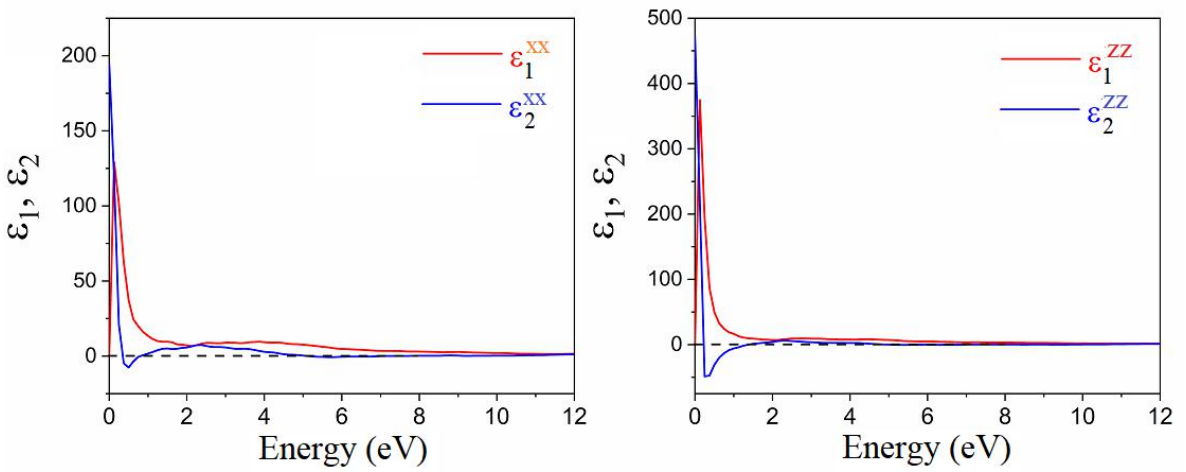

Fig. 8. The calculated reel and imaginary parts of dielectric functions for the $CdMn_7O_{12}$ compound.

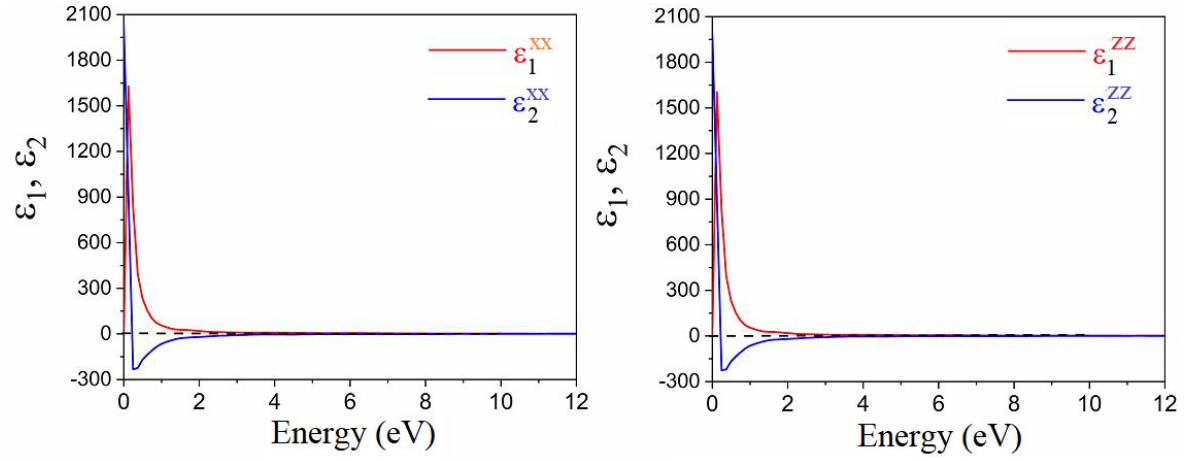

Fig. 9. The calculated reel and imaginary parts of dielectric functions for the $SrMn_7O_{12}$ compound.

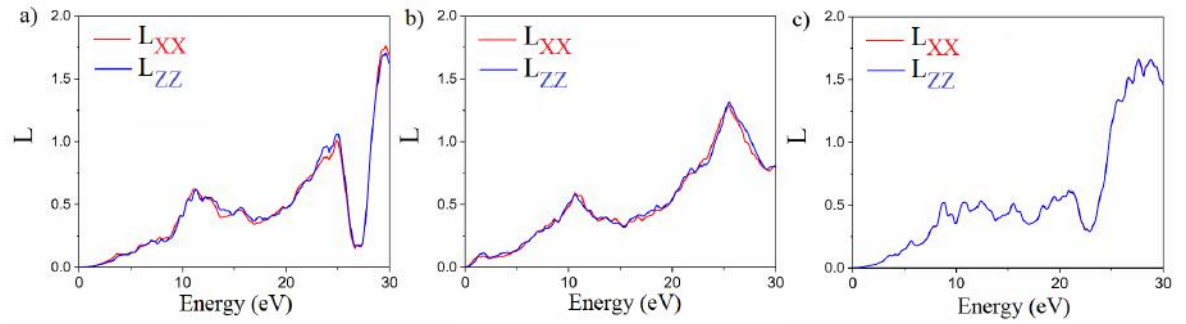

Fig. 10. The energy-loss spectrum (L) for a) $CaMn_7O_{12}$, b) $CdMn_7O_{12}$, and c) $SrMn_7O_{12}$.

When Figure 7-Figure 9 graphs are examined, it is determined that the value of ε_1 decreases with increasing energy between 0.12 and 0.38 eV in the $CaMn_7O_{12}$ compound, between 0.12 and 0.50 eV as well as 2.38 and 5.75 eV in the $CdMn_7O_{12}$ compound and between 0 and 0.38 eV and 9.75 and 10.36 eV in the $SrMn_7O_{12}$ compound. In these energy regions where the real part of the dielectric function decreases, anomalous dispersion characteristics are observed. In cases where the energy is zero (E=0 eV), $\varepsilon(\omega) = \varepsilon_1(0)$. Here, $\varepsilon_1(0)$ is the static dielectric constant. The calculated static dielectric constants for $CaMn_7O_{12}$, $CdMn_7O_{12}$, and $SrMn_7O_{12}$ compounds in the x(z) directions are 2610.8 (3302.3), 195.0 (472.27), and 2030.4 (2003.2), respectively. As seen in the Figure 7-Figure 9 graphs, the significant peak values of the imaginary part of the dielectric function are approximately in the 0-1 eV region. The maximum peak values (ε_2^{maks}) of the imaginary part of the dielectric function for the $CaMn_7O_{12}$, $CdMn_7O_{12}$, and $SrMn_7O_{12}$ compounds were determined as 0.372, 0.249 and 0.123 eV, respectively. It is seen that ε_2 increases until these peak values, and then it decreases. In this energy range, where ε_2 has significant peak values, there is a lot of contribution to the interband transitions. As indicated in the Figure 4-Figure 6 PDOS graphs, these energy regions where the interband transition is very high correspond to relatively strong p-d hybridization (O 2p-Mn 3d).

Plasmon vibrations occur in energy states where ε_1 part of the dielectric function is 0 eV and ε_2 part is minimum. The energy regions where plasmon

vibrations occur are associated with the collective vibrations of valence electrons and energy losses are maximum in these regions [43]. For the rhombohedral AMn_7O_{12} (A=Ca, Sr, Cd) compounds, energy loss functions (L) in the x- and z-directions were calculated using the $L(w) = \varepsilon_1(w)/(\varepsilon_1^2 + \varepsilon_2^2)$ equation. The calculation results are given in Figure 10. In the L_X and L_Z function plots for all three compounds, sharp maxima are observed above approximately 11 eV, 25 eV, and 25 eV. Plasmon vibrations are observed in these energy regions where energy losses are maximum.

4. CONCLUSION

We have performed the structural, mechanical, electronic, and optical properties of rhombohedral AMn_7O_{12} (A=Ca, Cd, and Sr) perovskite compounds using spin polarized generalized gradient approximation. The elastic constants calculated for AMn_7O_{12} (A=Ca, Cd, Sr) compounds provide the Born stability criteria. Using the calculated elastic constants, first the bulk and shear modulus values of AMn7O12 (A=Ca, Cd, Sr) compounds were calculated and then the other quantities were calculated. From the calculated elastic modulus values, it is determined that the $SrMn_7O_{12}$ compound is a harder material than the other compounds. In all three compounds the ionic contribution is dominant and these materials are ductile. Compared to the other two compounds, ionic contribution and ductility are higher in $CdMn_7O_{12}$. Among the calculated isotropic factor values, $CdMn_7O_{12}$ compound has the most anisotropic character. In the spin polarized state, all three compounds are semi-metals. The E_g values calculated from the spin up and spin down band graphs for the $CaMn_7O_{12}$, $CdMn_7O_{12}$, and $SrMn_7O_{12}$ compounds are 1.277 eV (indirect, in the spin down state), 0.917 eV (direct in the spin up state), and 2.214 eV (direct in the spin down state), respectively. The real and imaginary parts of the frequency dependent dielectric function along the x and z axes as well as the energy loss functions are calculated and interpreted.

ACKNOWLEDGEMENTS

This work is supported by the projects DPT-HAMIT and NATO-SET-193. One of the authors (Ekmel Ozbay) acknowledges partial support from the Turkish Academy of Sciences.

[1] *P. Jain, J. Saha, L.C. Gupta, S. Patnaik, A.K. Ganguli, R. Chatterjee.* 2017. Dramatic variation of the multiferroic properties in Sr doped $Ca_{1-x}Sr_xMn_7O_{12}$. *AIP Advances,* 7, 055832.

[2] *Y.S. Glazkova, N. Terada, Y. Matsushita, Y. Katsuya, M. Tanaka, A.V. Sobolev, I.G. Presniakov, A.A. Belik.* 2015. High-pressure synthesis, crystal structures, and properties of $CdMn_7O_{12}$ and $SrMn_7O_{12}$ perovskites. *Inorganic Chemistry*, 54, 90881–9091.

[3] *A.A. Belik, Y.S. Glazkova, Y. Yatsuya, M. Tanaka, A.V. Sobolev, I.A. Presniakov.* 2016. Low-temperature structural modulations in $CdMn_7O_{12}$, $CaMn_7O_{12}$, $SrMn_7O_{12}$, and $PbMn_7O_{12}$ perovskites studied by synchrotron X-ray powder diffraction and Mössbauer spectroscopy. The *Journal of Physical Chemistry C*, 120, 8278−8288.

[4] *B. Bochu, J.L. Buevoz, J. Chenavas, A. Collomb, J.C. Joubert, M. Marezio.* 1980. Bond lengths in '$CaMn_3$'$(Mn_4)O_{12}$: A new Jahn-Teller distortion of Mn^{3+} octahedra. *Solid State Communications*, 36, 133−138.

[5] *N.J. Perks, R.D. Johnson, C. Martin, L.C. Chapon, P.G. Radaelli.* 2012. Magneto-orbital helices as a route to coupling magnetism and ferroelectricity in multiferroic $CaMn_7O_{12}$. *Nature Communications*, 3, 1277−1282.

[6] *S. Kamba, V. Goian, F. Kadlec, D. Nuzhnyy, C. Kadlec, J. Vít, F. Borodavka, I.S. Glazkova, A.A. Belik.* 2019. Changes in spin and lattice dynamics induced by magnetic and structural phase transitions in multiferroic $SrMn_7O_{12}$. *Physical Review B*, 99, 184108.

[7] *H. Guo, M.T. Fernández-Díaz, L. Zhou, Y. Yin, Y. Long, A.C. Komarek.* 2017. Non-collinear magnetic structure of manganese quadruple perovskite $CdMn_7O_{12}$. Scientific Reports, 7, 45939.

[8] *G. Zhang, S. Dong, Z. Yan, Y. Guo, Q. Zhang, S. Yunoki, E. Dagotto, J.M. Liu.* 2011. Multiferroic properties of $CaMn_7O_{12}$. *Physical Review B*, 84, 174413.

[9] *R.D. Johnson, L.C. Chapon, D.D. Khalyavin, P. Manuel, P.G. Radaelli, C. Martin.* 2012. Giant improper ferroelectricity in the ferroaxial magnet $CaMn_7O_{12}$. *Physical Review Letters*, 108, 067201

[10] *M. Marezio, P.D. Dernier, J. Chenavas, J.C.J. Joubert. 1973.* Pressure synthesis and crystal structure of $NaMn_7O_{12}$. *Solid State Chemistry*, 6, 16−20.

[11] *H.M. Liu, S. Dong, Z.Z Du, P. Chu, J.M. Liu.* 2014. Giant electronic polarization induced by a helical spin order in $SrMn_7O_{12}$: First-principles calculations. EPL, 108, 67012.

[12] *G. Kresse, J. Hafner*. 1993. Ab initio molecular dynamics for liquid metals. *Physical Review B*, 47, 558 (R).

[13] G. *Kresse, J. Furthmüller*. 1996. Efficiency ab-initio total energy calculations for metals and semiconductors using a plane-wave basis set. *Computational Materials Science*, 6, 15-50.

[14] *G. Kresse, D. Joubert.* 1999. From ultrasoft pseudopotentials to the projector augmented-wave method. *Physical Review B*, 59, 1758.

[15] *G. Kresse, J. Furthmüller.* 1996. Efficient iterative schemes for ab initio total- energy calculations using a plane-wave basis set. *Physical Review B*, 54, 11169.

[16] *P. Hohenberg, W. Kohn.* 1964. Inhomogeneous Electron Gas. Physical Review, 136, A1133.

[17] *J.P. Perdew, K. Burke, M. Ernzerhof.* 1996. Generalized gradient approximation made simple. *Physical Review Letters*, 77, 3865.

[18] *H.J. Monkhorst, J.D. Pack.* 1976. Special points for Brillouin-zone integrations. *Physical Review B*, 13, 5188.

[19] *B. Bochu, J. Chenavas, J. C. Joubert, M. Marezio.* 1974. High pressure synthesis and crystal structure of a new series of perovskite-like compounds CMn_7O_{12} (C = Na, Ca, Cd, Sr, La, Nd). *Journal of Solid State Chemistry*, 11, 88-93.

[20] *W. Sławin´ski, R. Przeniosło, I. Sosnowska, M. Bieringer, I. Margiolakic, E. Suard.* Modulation of atomic positions in $CaCu_xMn_{7-x}O_{12}$ ($x < 0.1$). *Acta Crystallographica*, B65, 535–542.

[21] *J. Sannigrahi, S. Chattopadhyay, D. Dutta, S. Giri, S. Majumdar.* 2013. Magnetic and electric properties of $CaMn_7O_{12}$ based multiferroic compounds: effect of electron doping. *Journal of Physics: Condensed Matter*, 25, 246001.

[22] *R.D. Johnson, L.C. Chapon, D.D. Khalyavin, P. Manuel, P.G. Radaelli, C. Martin.* 2012. Giant Improper Ferroelectricity in the Ferroaxial Magnet $CaMn_7O_{12}$. *PRL*, 108, 067201.

[23] *H. Koc, E. Deligoz, Amirullah M. Mamedov.* 2011. The elastic, electronic, and optical properties of PtSi and PtGe compounds. *Philosophical Magazine*, 91, 3093–3107.

[24] *Y.L Page, P. Saxe.* 2001. Symmetry-general least-squares extraction of elastic coefficients from ab initio total energy. *Physical Review B*, 63, 174103.

[25] *J.J. Wang, F.Y. Meng, X.Q. Ma, M.X. Xu, L.Q. Chen.* 2010. Lattice, elastic, polarization, and electrostrictive properties of from first-principles. *Journal of Applied Physics*, 108, 034107.

[26] *W. Voight.* 1928. Lehrbook der kristallphysik, Leipsig: Teubner, pp. 962.

[27] *A. Reuss.* 1929. Berechnung der fließgrenze von mischkristallen auf grund der plastizitatsbedingung für einkristalle. *Zeitschrift für Angewante Mathematik und Mechanik*, 9, 49-58.

[28] *R. Hill*. 1952. The elastic behavior of crystalline aggregate. *Proceedings of the Physical Society Section A*, 65, 349-354.

[29] *W. Liu, Y.D. Gan, F.S. Liu, B. Tang, S.H. Zhu, Q.J. Liu.* 2022. First-principles study of sructural, electronic, and elastic properties of Sb_2S_3 under pressure. *Physics Status Solidi* B, 259, 2100234.

[30] *V.V. Bannikov, I.R. Shein, A.L. Ivanovskii.* 2007. Electronic structure, chemical bonding and elastic properties of the first thorium-containing nitride perovskite $TaThN_3$. *Physica Status Solidi (RRL)*, 3, 89-91.

[31] H. Koc, A. Yildirim, E. Tetik, E. Deligoz. 2012. Ab initio calculation of the structural, elastik, electronic, and *linear optical properties of ZrPtSi and TiPtSi ternary compounds. Computational Materials Science, 62, 235-242.*

[32] *H. Koc, A.M. Mamedov, E. Deligoz, H. Ozisik.* 2012. First principles prediction of the elastic, electronic, and optical properties of Sb_2S_3 and Sb_2Se_3 compounds. *Solid State Science*, 14, 1211-1220.

[33] *I.R. Shein, A.L. Ivanovskii*. 2008. Elastic properties of mono- and polycrystalline hexagonal AlB_2-like diborides of s, p and d metals from first-principles calculations. *Journal of Physics: Condensed Matter*, 20, 415218.

[34] *F. Pogh.* 1954. Relations between the elastic moduli and the plastic properties of polycrystalline pure metals. *Philosophical Magazine*, 45, 823-843.

[35] *P. Ravindran, L. Fast, P.A. Korzhavyi, B. Johansson, J. Wills, O. Erikson.* 1998. Density functional theory for calculation of elastic properties of orthorhombic crystals: application to $TiSi_2$. *Journal of Applied Physics*, 84, 4891-4904.

[36] *H. Zhai, X. Li, J. Du.* 2012. First-principles calculations on elasticity and anisotropy of tetragonal tungsten dinitride under pressure. *Materials Transactions*, 53, 1247-1251.

[37] *D.H. Chung, W.R. Buessem.* 1968. In: Vahldiek FW, Mersol SA, editors: Anisotropy in single crystal refractory compounds, New York: Plenum, p 217.

[38] *O.L. Anderson.* 1963. A simplified method for calculating the Debye temperature from elastic constants. *Journal of Physics and Chemistry of Solids*, 24, 909-917.

[39] *I. Johnston, G. Keeler, R. Rollins, S. Spicklemire.* 1996. Solids state physics simulations, the consortium for upper level physics software, New York: Wiley.

[40] *E. Schreiber, O.L. Anderson, N. Soga.* 1973. Elastic constants and their measurements, New York: McGraw-Hill.

[41] *H.R. Philipp, H. Ehrenreich.* 1963. Optical properties of semiconductors. *Physical Review*, 129, 1550-1560.

[42] *H. Koc, A.M. Mamedov, E. Deligoz, H. Ozisik.* 2012. First principles prediction of the elastic, electronic, and optical properties of Sb_2S_3 and Sb_2Se_3 compounds. *Solid State Sciences*, 14, 1211-1220.

[43] *L. Marton.* 1956. Experiments on low-energy electron scattering and energy losses. *Reviews of Modern Physics*, 28, 172-183.